Numerical Investigation of a Jet and Vortex Actuator (JaVA)

Muhammad Aqeel Rashad and Ulrich Rist

Institut für Aerodynamik & Gasdynamik (IAG), Pfaffenwaldring 21, 70550 Stuttgart, Germany
[rashad]/[rist]@iag.uni-stuttgart.de

Summary

In the present study an active flow control actuator is studied numerically using the CFD package Fluent®. A two-dimensional setup is chosen which corresponds to a cut through the actual configuration that was studied experimentally by Lachowicz *et al.* [1] and called "Jet and Vortex Actuator" (JaVA) because of its ability to produce such completely different flow regimes when its actuation frequency and amplitude are changed. Three cases are selected for validation of the simulations. A vortex mode, a vertical jet and a wall-jet mode. Our simulations yield the *unsteady* flow field, whereas only time-averaged data are available from literature. Thus, our simulations provide extra details of the flows through the gaps intended for a better understanding of the actuator flow. Qualitative and quantitative comparisons of the time-averaged data with the experiments are very encouraging. Especially, the different flow regimes appear for the same parameters as in the experiments.

1 Introduction and Background

Actuator flow control can be of two kinds: passive and active. A passive or conventional flow control actuator has the disadvantage that it is designed only for a specific (flight) condition and also it produces parasitic drag in steady cruise condition. Active flow control actuators minimize both these disadvantages. These actuators can be used in multiple flight conditions in contrast to passive flow control devices. Furthermore, active flow control actuators produce negligible drag when the system is not actuated.

The current JaVA system evolved from an earlier flow actuator developed by Jacobson & Reynolds [2]. This actuator consists of a cantilevered beam oscillating in a cavity. The plate was placed asymmetrically within the cavity to form wide and narrow gaps when viewed from the top of the plate. A periodically emerging jet, from the narrow slot, generated longitudinal vortical disturbances when interacting with a boundary layer in a water tunnel. In the wake of a small circular cylinder placed in a laminar boundary layer the actuator system delayed transition by about 40 displacement thicknesses. Koumoutsakos [4] conducted a parametric numerical study of an actuator with no external flow. Instead of simulating the motion of

a cantilevered beam, piston-type motion was simulated in order to determine the fundamental physical mechanisms responsible for disturbance generation from the actuator; note that the motion of the JaVA is also of piston-type. For a given slot width, Koumoutsakos showed that at relatively high frequencies a periodic jet developed from the narrow slot, while at relatively low frequencies, the periodic jet developed from the wide slot. This suggested that the actuator slot flow is Stokes number dependent. However, Saddoughi *et al.* [5] conducted a series of experiments using a cantilevered-beam type actuator with the same Stokes number as Jacobson & Reynolds [2]. It was found that the flow patterns in the two experiments were qualitatively different. Thus, similar to the study of Koumoutsakos, a more basic actuator motion, the piston-type motion, is used in this study to better understand the actuator flow physics.

The active flow control actuator under consideration is from Lachowicz *et al.* [1], consists of a cavity and a rigid plate that is placed at the top of the cavity such that it forms a narrow and a wide gap when viewed from the top, see Fig. 1. The plate is oscillated in the vertical direction such that the plate motion is uniform along its length and width. The actuator plate acts like a piston pumping air out of the cavity on the downstroke and sucking air into the cavity on the upstroke. This kind of active flow control actuator produces different flow fields (free jet, wall jet, and vortex flow) and this type of actuator will be characterized. The flow field will be computed and visualized by varying the amplitude and frequency of oscillation. An angled jet is produced at relatively low amplitude and frequency from the wide gap while at relatively high amplitude and low frequency a free jet is produced from the wide gap. As the frequency is increased at low amplitude a wall jet is produced from the wide gap directing towards the narrow gap. The wall jet is primarily horizontal near the narrow gap and is characterized by steady horizontal flow pumping from the wide gap towards the narrow gap end. Such actuators may be used to energize the boundary layer by accelerating the fluid tangentially near the wall surface. As the amplitude is increased from the wall jet regime and at high frequency a vortex is generated at the wide gap. The vortex regime may be used to promote mixing and suppress boundary layer separation.

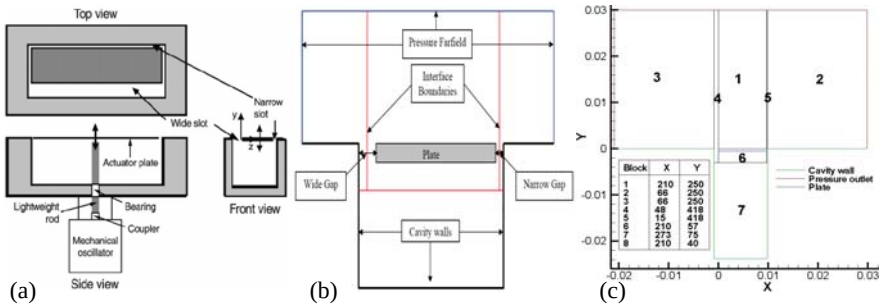

Figure 1 (a) Basic setup of the JaVA; (b) Geometry and boundary conditions; (c) Number of grid points used in each block.

2 Grid, Boundary Conditions and Numerical Approach

For the present actuator-geometry and boundary conditions the grid generator GAMBIT is used, see Fig. 1. For the flow calculations and visualization use of the general purpose CFD software Fluent® from Fluent Inc. seemed to be the most appropriate, because of the need for simulating rather complex geometries with moving boundaries and grids at different unsteady flow speeds. This software appears to be well-suited because of its versatility to deal with dynamic meshes. We use structured deformable dynamical grids with sliding interfaces between different blocks where necessary. For the specification of problem-specific boundary conditions Fluent uses the concept of *"user-defined functions"*, i.e. the user has to specify his/her boundary conditions in a C-like syntax as a function that is bound to the executable upon execution. This is very flexible and general. However, not always free of errors. In some cases it turned out that it is not sufficient to simply specify wall motions (with the idea that this will automatically drive the flow via appropriate boundary conditions). Unexpectedly, it was necessary to specify extra boundary conditions for the fluid on the moving boundaries. This adds extra flexibility, like consideration of permeable walls, for instance, but careful checks are necessary in order to verify use of appropriate boundary conditions for a given problem. In the present application the blocks attached to the actuator plate (nos. 1 and 6 in Fig. 1c) are moved with the help of *user-defined functions* in Fluent. Since only two-dimensional measurements are available with Lachowicz *et al.* [1] and the flow field in the middle of the actuator is considered to be two-dimensional (if placed in still air, i.e. without a free stream flow in the plane-normal direction), we begin with two-dimensional simulations for comparison but three-dimensional simulations are performed as well.

The motion of the plate is prescribed by the following set of equations

$$\begin{aligned} \omega &= 2\pi f, & T &= 1/f, \\ x(t) &= a\sin(\omega t), & v(t) &= \dot{x}(t) = a\omega\cos(\omega t), \end{aligned}$$

where f is the actuator-plate vibration frequency, T the oscillation period, a the actuator-plate amplitude, and v the actuator-plate velocity.

3 Results

3.1 Case 1, Vortex Mode

The first simulation is performed for a scaled frequency (Strouhal number) $\mathrm{Sr} = fb/v_{max} = b/2\pi a = 5.47$ and a scaled amplitude $S_a 2\pi a/b = 0.1829$, where b is the plate width. In this case a big vortex is produced above the plate over the wide gap. A secondary weaker vortex is also present towards the narrow gap. In addition, we also observe a small and a large vortex inside the cavity. With many simulations it is observed that the size of the vortex is mesh dependent. So, special care is required to get a mesh-independent vortex. Fig. 2 (c and d) shows the contours of mean velocity magnitude averaged over the last four oscillation periods (22^{nd} to 25^{th})

and these are compared with Lachowicz *et al.* [1] and Joslin *et al.* [3] in subfigures a and b. The qualitative comparison with the stream lines provided by Lachowicz *et al.* [1] and Joslin *et al.* [3] in Fig. 2 turns out to be excellent. Comparing the size of the vortex with respect to the width of the actuator it appears that the size of vortex in our case is almost of the same size as observed in the experiments [1].

A quantitative comparison of time-averaged velocity profiles along a vertical cut through the vortex centre is shown in Fig. 3a. This comparison once again shows that the vortex size in our case is almost equal to the one observed by Lachowicz *et al.*. The quantitative agreement of the positive and negative velocity magnitude maxima agrees much better with the experimental results than the results of the numerical modelling performed by Joslin *et al.* [3]. Fig. 3b shows the plots of instantaneous velocity in the wide gap for eight different phases of the oscillation. It can be seen that the flow is very complex. There is flow separation and reversed flow. The reason of this complex flow behaviour is that the wide gap width is very large compared to the plate thickness. We now turn to the narrow gap in Fig. 3c, which shows the plots of instantaneous velocity in the narrow gap for eight different phases of oscillation. Here, the flow is more like a mixed *Couette-Poiseuille* flow, simply because the narrow gap width is very small compared to the plate thickness. Another typical observation (for oscillating viscous flows) in this figure is that the velocity profiles are not symmetric during outward and inward flow. Furthermore the maximal outflow velocity does not occur in phase with the plate oscillation. It occurs about 45^o after the plate has reached its upper or lower turning point ($\Theta = 90^o$ or $\Theta = 270^o$). The green curve at $\Theta = 90^o$ does not return to zero at the right end. This is simply because for the present set-up, the actuator plate has moved outside the cavity at this time instant and there is no longer a wall at $x > 0.00979$. There is no such phase shift in the wide gap as observed in Fig. 3b.

3.2 Case 2, Free Jet Mode

According to Lachowicz [1] at lower frequency and high scaled amplitude we should expect a free jet at the wide gap. In this case we did simulations for Sr $= 5.30$ and $S_a = 0.19$. With this frequency and scaled amplitude we get a free jet from the wide gap which is slightly tilted towards the narrow gap.

Our quantitative information is presented in Fig. 4 using contours of mean velocity magnitude. The results are averaged for the last four time periods. The velocity field confirms that we get a free jet from the wide gap which begins in vertical direction before it bends somewhat to the right. In addition, once again we observe a small and a large vortex inside the cavity. Continuing the simulation to later times, straightens the jet further, such that the picture of an inclined jet becomes clearer. This figure also compares our results with the one published from the experiments. Here, frequency and scaled amplitude are the same as those given in [1] for their experiments. Thus, there is a very good agreement between the two results. Unfortunately, there is no quantitative data available for this mode of actuator to compare the results.

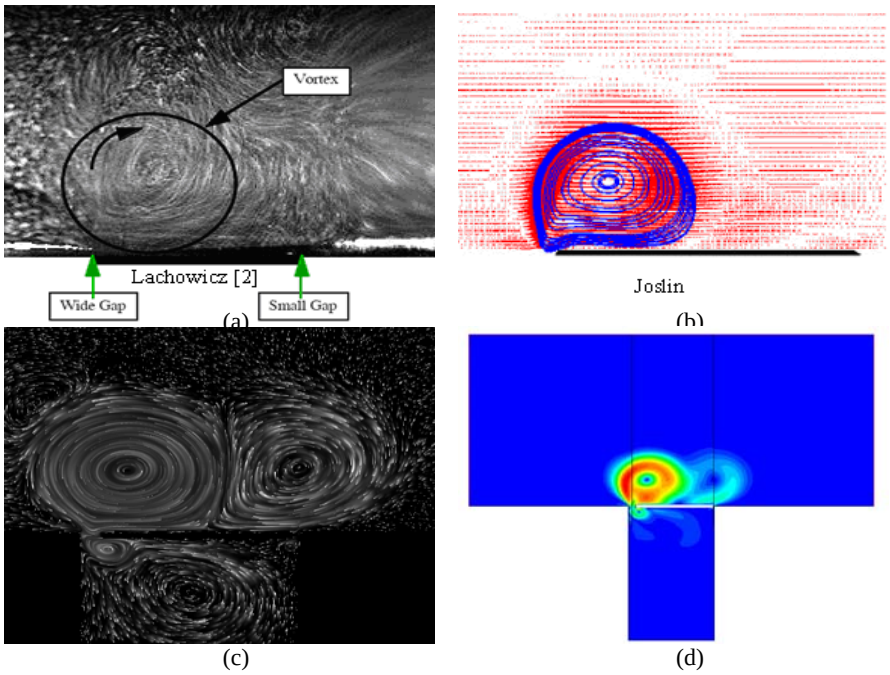

Figure 2 Velocity contours. (a) Lachowicz *et al.* [1]; (b) Joslin *et al.* [3]; (c and d) Fluent.

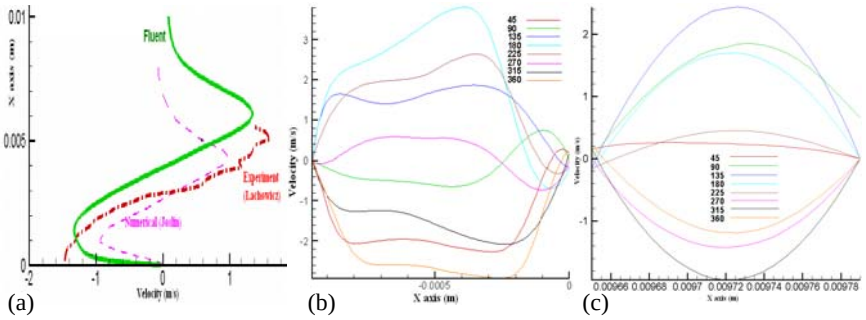

Figure 3 (a) Comparison of velocity profiles through vortex centre; (b) Velocities in the wide gap; (c) Velocities in the narrow gap.

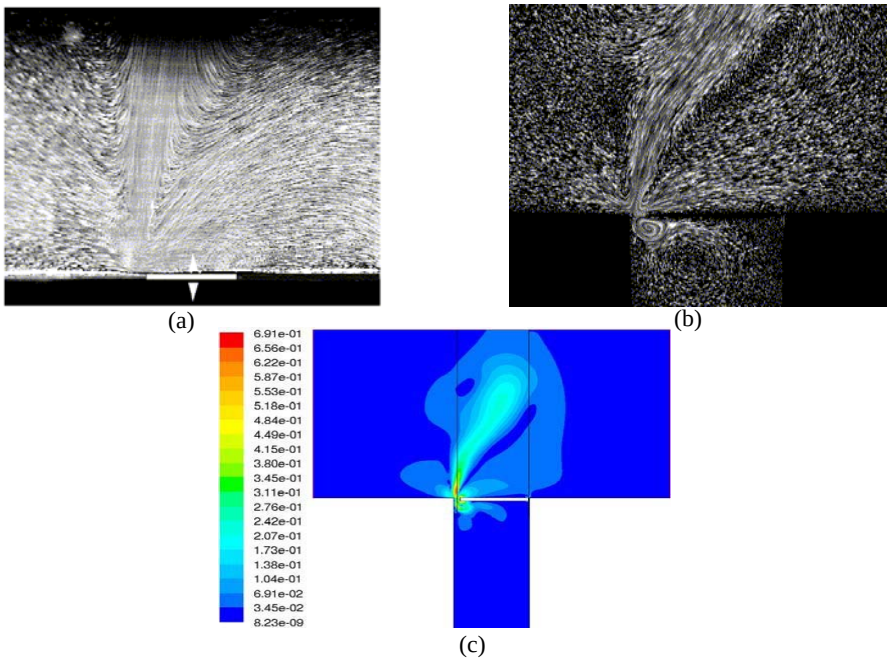

Figure 4 Velocity contours. (a) Lachowicz *et al.* [1]; (b and c) Fluent.

3.3 Case 3, Wall Jet Mode

According to Lachowicz *et al.* [1] at low scaled amplitude and high frequency we should expect a wall jet pumping fluid from the wide gap to the narrow gap. Therefore, we increased the Strouhal number to Sr $= 9.03$ and reduced the scaled amplitude to $S_a = 0.11$ at the same time. In this case we observe a wall jet from the wide to the narrow gap, i.e., the same qualitative feature as in [1] and this is shown in Fig. 5 where we compare the two averaged flow fields using stream lines. A counter-clockwise rotating vortex sits above the narrow gap. In the experiment the flow towards the actuator on the left of the vortex appears clearer than in the numerical simulation but this is merely an effect of different integration times of the streamline segments. The next difference is that the wall jet continues far beyond the actuator region to the right in the experiment which is less pronounced in the simulation. Here, a continuation of the simulation could extend the jet further to the right.

Again, there is no quantitative data available for this mode of actuator to compare with our results. We represent time-averaged results in Fig. 5c to confirm our interpretation of the streamlines. The velocity magnitude indicates rather clearly that the results are still under the influence of the start-up transient of the simulation.

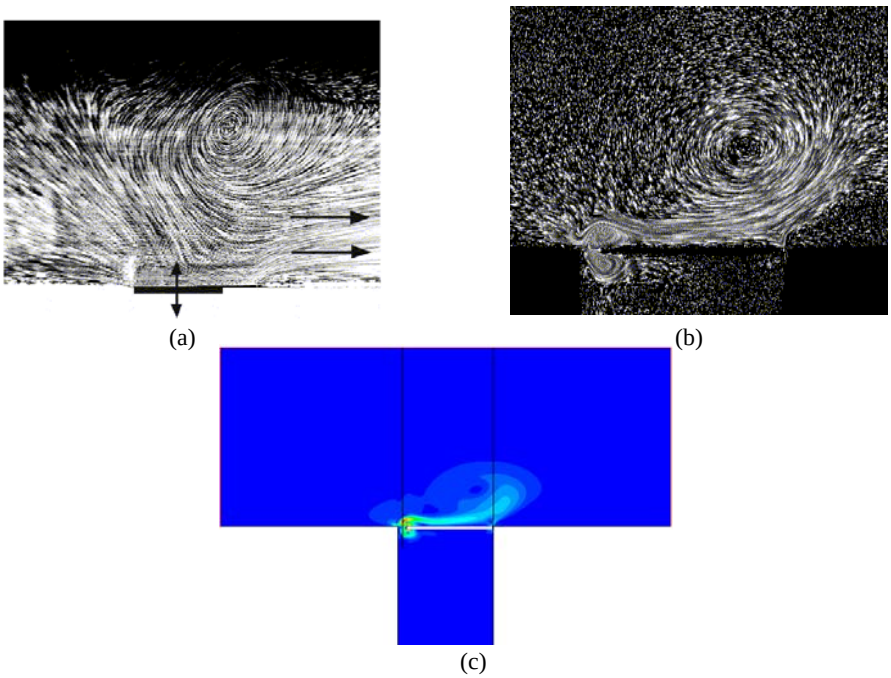

Figure 5 Velocity contours. (a) Lachowicz *et al.* [1]; (b and c) Fluent.

4 Conclusions

Three different simulations have been performed to show the effects of diverse parameters which influence the flow field. Vertical jet, wall jet, and vortex modes of actuation of the actuator have been detected and compared to available previous results where possible.

In general, it turns out that our simulation methodology is capable of reproducing the observations by Lachowicz *et al.* to full extent. However, discretisation of the computational grid needs some care because the size of the observed vortex can depend on insufficient grid resolution. In other cases it was observed that the jet direction may also depend on resolution. We had also compared the different flow regimes with Lachowicz *et al.* [1] see Fig. 6. The Reynolds number in this figure is $Re = v_{max} b/\nu = 2\pi f a b/\nu$.

For the JaVA design three-dimensional simulations have been started as well. These will be used to study side-wall effects due to the finite extend of the actuator in reality. This is an undocumented feature of the JaVA that deserves attention. Finally, the actuator must be coupled to boundary layer flows in order to assess its efficiency for flow control.

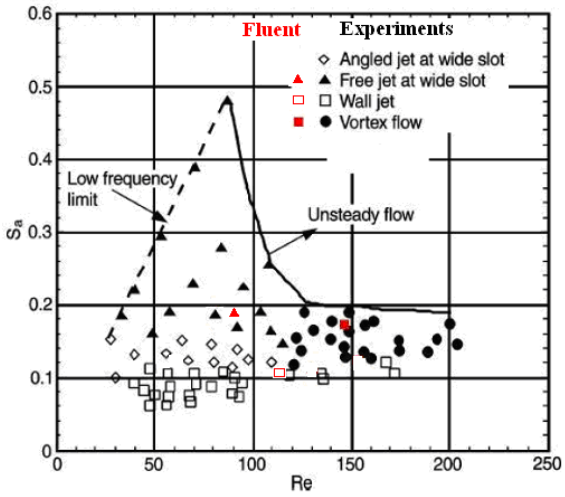

Figure 6 Comparison with experimentally observed flow regimes from Lachowicz *et al.* [1].

Acknowledgements

We gratefully acknowledge financial support for the present research provided by Airbus.

References

[1] J.T. Lachowicz, C. Yao, R.W. Wlezien: “Flow field characterization of a jet and vortex actuator”, Exp. Fluids **27**, 1999, pp. 12-20.

[2] S.C. Jacobson, W.C. Reynolds: “Active control of streamwise vortices and streaks in boundary layers”, J. Fluid Mech. **360**, 1998, pp. 179-994.

[3] R.D. Joslin, J.T. Lachowicz, C. Yao: “DNS of flow induced by a multi-flow actuator”, ASME FEDSM98-5302, ASME Fluid Engineering Meeting, 1998.

[4] P. Koumoutsakos: “Simulations of vortex generators”, Center for Turbulence Research, Annual Research Briefs, 1995, pp. 233-240.

[5] S.G. Saddoughi, P. Koumoutsakos, P. Bradshaw, N.N. Mansour: “Investigation of ‘On Demand’ vortex generators”, Center for Turbulence Research Manuscript No. 171, 1998, Stanford University.